Research Article | Vol. 27, No. 21 / 14 October 2019 / Optics Express 30421

Optics EXPRESS

Highly sensitive and selective optical sensor for lead ion detection based on liquid crystal decorated with DNAzyme

XIAOFANG NIU, YANJUN LIU, FEI WANG, AND DAN LUO*

Department of Electrical and Electronic Engineering, Southern University of Science and Technology, Xueyuan Road 1088, Nanshan District, Shenzhen, Guangdong, 518055, China
*luod@sustech.edu.cn

Abstract: Lead ions (Pb^{2+}) are one of the major environmental pollutants that are dangerous for human health, thus the detection methods of Pb^{2+} become very important as well. However, most reported techniques suffer from drawbacks such as long time, expensive equipment and complicated testing process, which prevent the use of real-time application. Herein, we demonstrate a novel liquid crystal optical sensor for detection of Pb^{2+} based on DNAzyme and its combined strand. The ordered and disordered configuration of liquid crystals, induced by complementary DNA strand and catalytically cleaved DNA in presence of lead ion separately, leads to dark and bright optical image under POM. The proposed naked-eye optical sensor possesses an extremely broad detection range of Pb^{2+} from 50 nM to 500 μM, with a low detection limit about 36.8 nM. The sensor also demonstrates high selectivity of Pb^{2+} from many other metal ions. The proposal LC sensor is highly sensitive and selective for Pb^{2+} detection, which provides a novel platform for other heavy metal, DNAs or antigen in biological and chemical fields by modifying sensing molecules.

1. Introduction

The quality deterioration of heavy metal ions in natural environment has become a major global issue. With developed of industry and technology, more and more metal ions have been continuously released [1,2]. Excess heavy metal ions can be a hazard in drinking water directly the aquatic ecosystem and human health [3]. Lead ions (Pb^{2+}) are one of the major environmental pollutants that are dangerous for human health including memory loss, muscle paralysis, mental troubles, and cardiovascular dysfunction [4,5]. Therefore, sensitive and quantitative detection of lead ions is quite important. Several methods have been developed for the detection of lead ions, such as inductively coupled plasma atomic emission spectroscopy (ICP-AES) [6], atomic absorption spectroscopy (AAS) [7,8], surface plasmon resonance (SPR) [9], colorimetric [10,11], biochemical [12] and electrochemical techniques [13,14]. However, these analytical methods require highly expensive instruments, cumbersome operating conditions and time-consuming pretreatments. Therefore, it is highly desirable to develop novel method for Pb^{2+} real-time detection. As a naked-eye optical sensor, liquid crystals (LCs) based optical sensor has attracted significant attention due to its fast, low-cost, and simplicity [15]. The naked-eye LC optical sensor for Pb^{2+} detection is a promising technique in clinical toxicology, environmental monitoring and industry process monitoring applications.

In recent years, liquid crystals have attracted a lot of interests in chemical [16], material [17] and biological fields [18] due to their unique optical and optoelectronic properties. The liquid crystal is extraordinary sensitive to physical and chemical properties of a bounding interface due to the transduction ability of molecular events at interface [19–21]. LC based sensor has been widely used in various chemical analysis and biosensors. Abbott et al. reported the measurement of chemical exposure based on recognition-driven anchoring transitions in LC, and then they

#375943 https://doi.org/10.1364/OE.27.030421
Journal © 2019 Received 21 Aug 2019; revised 28 Sep 2019; accepted 29 Sep 2019; published 7 Oct 2019

Optics EXPRESS

demonstrated the gas sensors using metal salt immobilized liquid crystals [22]. Several research works have been demonstrated to utilize nematic liquid crystals such as 5CB for detection of bacteria [23,24], viruses [25], cancer cells and protein [26], polymer chemicals [27] and heavy metal ions [28].

Herein, we developed a liquid crystal optical sensor for detection of Pb^{2+} based on DNA degradation. The mechanism of detection is due to the disturbance of ordered liquid crystals configuration induced by adding Pb^{2+}. The proposed LC optical sensor possesses a wide detection range with low detection limit, and a high selectivity, which leads to a quickly, simply and low-cost quantitative analysis of Pb^{2+}.

DNAzyme (catalytic strand), as the main member of functional nucleic acids, is reported to recognize metal ions, due to the capability of either binding to a target molecule or performing catalytic reactions [29]. In 2003 Brown reported a DNAzyme that was used for binding Pb^{2+} and result in catalytic hydrolysis. Several types of DNAzyme based Pb^{2+} sensor have been reported. DNAzyme has been for binding Pb^{2+} and resulting in catalytic hydrolysis of the nucleic acids [30]. A colorimetric sensor by utilizing Pb^{2+} induced allosteric G-quadruplex DNAzyme for detection the Pb^{2+} was developed [31]. Both electrochemical and photoelectrochemical DNAzyme sensor for detection of Pb^{2+} have been demonstrated [32]. "Turn on" fluorescence sensor based on graphene quantum dots and gold nanoparticles has also been studied [33]. In this study, DNAzyme and its combined strand were used for LC based optical Pb^{2+} sensor. Figure 1(a) depicts the fabrication process of the Pb^{2+} sensor based on liquid crystals. Firstly, a glass slide was modified with N, Ndimethyl-N-octadecyl (3-aminopropyl) trimethoxysilyl chloride (DMOAP) and 3-aminopropyl-trimethoxysilane (APTES). The DMOAP was used to align liquid crystals (5CB) molecules perpendicularly to the surface of glass substrate through chemical bonds of molecules interactions [12], leading to a homeotropic configuration of liquid crystals on the glass slide. The APTES molecules were attached on the substrate surface of glass by covalent Si-O-Si bonds. It possessed plentiful of terminal amino groups, could catch specific anionic complementary DNA strands (the structural formula is shown in Fig. 1(b)) that consisted of catalytic strand (DNAzyme) and combined strand. Glutaraldehyde (GA) was subsequently added as the intermedia of APTES and DNA strand, where the amino groups in GA and APTES would cross linked with each other. Then a cationic surfactant dodecyl trimethyl ammonium

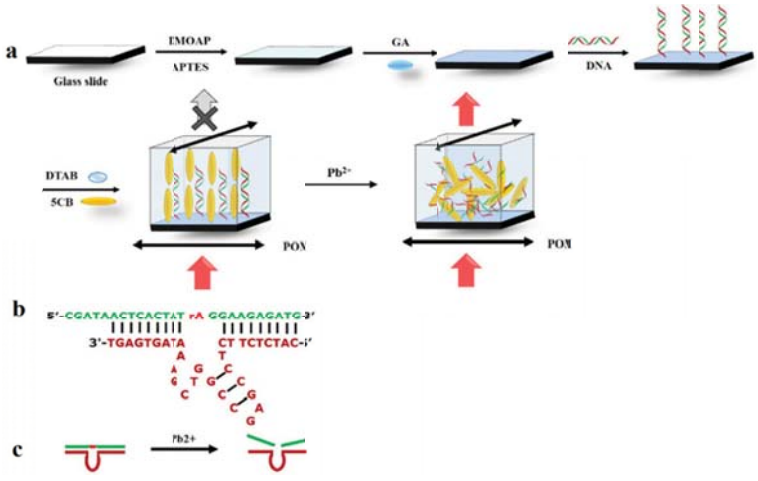

Fig. 1. (a) Schematic illustration of Pb2+ detection based on liquid crystals. (b) Structure formula of complementary DNA strands. (c) Schematic of catalytically cleave of the complementary DNA molecules.

Optics EXPRESS

bromide (DTAB) and nematic liquid crystal 5CB were added on the surface of glass slide. The DTAB (aqueous solution) molecules could bind to the DNA through electrostatic interaction [34], resulting in good dissolution of DNA in aqueous solution. It would form a self-assembly monolayer at the aqueous/LC interface and assist the alignment of LC molecules [35]. The liquid crystal 5CB molecules (as well as DNA strand) would perpendicularly align on the DMOAP coated glass substrate and form homeotropic configuration, leading to a dark optical image under polarizing optical microscope (POM). In appearance of Pb^{2+}, the complementary DNA strand would disassemble by catalytically cleaving of DNA molecules due to catalytic activity of catalytic strand. The DNA molecules would be catalytically cleaved at the "rA" site [34], unwinding the complementary DNA strand with nucleotide fragment, as shown in Fig. 1(c). The cleaved DNA strands would disturb the homeotropic orientation of LC 5CB, leading to a bright optical image under POM.

2. Materials and methods

In our experiment, sodium citrate solution, phosphate buffer solution (10 mM PBS, contained with Na_2HPO_4 and $NaHPO_4$, pH 7.4), $Pb(NO_3)_2$, $AgNO_3$, KCl, HgCl, $CuCl_2$, $MnCl_2$, $CaCl_2$, $ZnCl_2$, $CdCl_2$, DMOAP, APTES, DTAB and GA were all obtained from Sigma-Aldrich (St. Louis, USA). Liquid crystal 5CB was bought from HCCH (Jiangsu, China). The combined strand and catalytic strand were purchased from Shenggong Bioengineering (Shanghai, China), and glass slides (Sail brand) were purchased from Dongsheng Glass (Taizhou, China). Optical images were obtained by polarization optical microscope (Ti 200, Nikon). The catalytic strand (5'-NH_2-CGATAACTCACTATrAGGAAGAGATG-3'), and combined strand (5'-CATCTCTTCTCCGAGCCGGTCGAAATAGTGAGT-3') were purchased from Shenggong Bioengineering (Shanghai, China).

To fabricate the Pb^{2+} sensor, the glass slide was cleaned by sufficient piranha solution (1:1 30% H_2O_2 in H_2O:H_2SO_4; caution: piranha solution is exothermic and strongly reacts with organics) at 110°C for 30 min and then copiously rinsed with deionized water. After drying by nitrogen (N_2), the sample was immersed in ethanol solution that contained 0.1% (v/v) DMOAP and APTES for 30 min. Then, 0.5% GA was coated on the substrate and dried under N_2. Afterwards, the sample was immersed in a solution that contained 200 μM catalytic strand and 200 μM combined strands of DNA in 37°C for 1 h. Subsequently, the sample was rinsed with deionized water to clean unbonded DNA strands. Finally, transmission electron microscopy (TEM) grids were placed on the surface of glass slide and 1 μL of 5CB was dispensed onto each grid by dropping. Then, the 5CB-filled TEM grid was exposed in DTAB solution. All our experiments are carried on room temperature of 25°C. In our experiment, the thickness of LC is determined by the thickness of TEM grids, which is 10 μm.

3. Results and discussions

The concentration of DTAB plays an important role in alignment of liquid crystals with DNA strands in the initial state. Figure 2 shows the optical image of Pb^{2+} sensor sample under polarization optical microscopy (POM) at increase of DTAB from 0 M to 50 Mm. It can be seen that, when there was no DTAB (0 M), the optical image of sample was bright. The brightness decreased with the increase of concentration of DTAB, indicating that more and more LC molecules had been perpendicularly anchored on the glass slide. When the concentration of DTAB reached to 10 mM, the optical image of sample turned to almost totally dark except the edge of grid. Further increase of the concentration of DTAB up to 50 mM wouldn't significantly change the darkness of sample. It means that the alignment effect of DTAB saturates from 10 mM, where the cationic from DTAB and anionic from complementary DNA strand comes to anion-cation balance. In our experiment, the 10 mM of DTAB was chosen as the optimal concentration in following parts. In Fig. 2, the POM images of LC are measured in a stable status

Optics EXPRESS

(same time gap is used for keeping measure condition fixed) in different concentration of DTAB. The stable condition is also applied in Fig. 3 for influence of DMOAP.

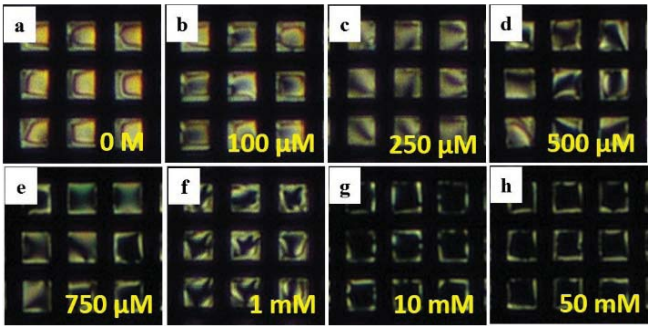

Fig. 2. Optical appearances of Pb^{2+} sensor sample under polarizing optical microscope with (a) 0 M, (b)100 µM, (c)250 µM, (d)500 µM, (e)750 µM, (f)1 mM, (g) 10 mM, and (h) 50 mM concentration of DTAB.

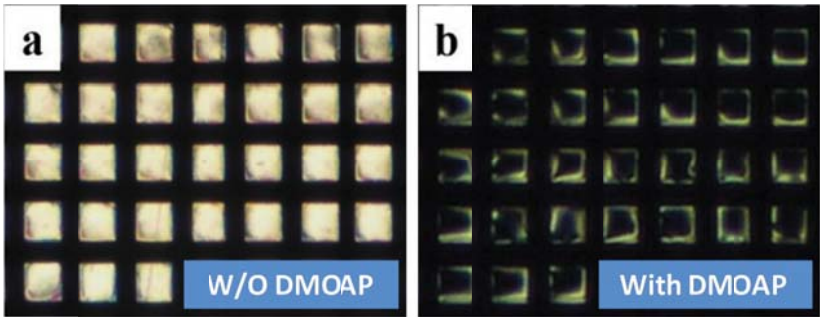

Fig. 3. POM image of sensor in case of (a) without DMOAP and (b) with DMOAP.

To study the influence of DMOAP for anchoring of 5CB molecules, two glass slides were used in comparison experiment, where one glass slide was modified with APTES/GA and another was modified with DMOAP/APTES/GA. Figure 3(a)–3(b) show the POM image of sample cell when the complementary DNA strand and 5CB was added in the LC cell in case of without DMOAP and with DMOAP, which corresponds to a bright and dark image, respectively. It is indicated that the DMOAP plays a great role of anchoring 5CB molecules in the strategy for forming the homeotropic configuration of LC molecular. In addition, it is worth noticing that the concentration (from 0 to 500 µM) of the complementary DNA strand has no significant effect on the anchoring of 5CB in our experiment.

To evaluate the analytical performance for quantitative analysis of Pb^{2+}, the effect of Pb^{2+} concentration on brightness of sensor POM image was investigated. Different concentration of Pb^{2+} (0-500 µM) solution was added into the optical sensor based on liquid crystal. Before the Pb^{2+} was added (Fig. 4(a)), the optical image was relatively dark, indicating a good homeotropic configuration of LC molecules. However, after the Pb^{2+} was added into the sensor, the complementary DNA strand would disassemble by catalytically cleaving of DNA molecules. The cleaved DNA strands would disturb the homeotropic orientation of LC 5CB, leading to a bright optical image under POM. The amount of cleave DNA strands depends on the concentration of Pb^{2+} added. With the increase of Pb^{2+}, more and more DNA strands were cleaved, resulting in a brighter optical image under POM. Therefore, the brightness could be used as the indicator

Optics EXPRESS

for the added concentration of Pb^{2+}. Figure 4(b)–4(h) shows the optical image of sensor under POM when concentration of Pb^{2+} was 50 nM, 150 nM, 500 nM, 1 μM, 50 μM, 250 μM and 500 μM, respectively. The relationship between optical image brightness and the logarithm of concentration of Pb^{2+} is plotted in Fig. 4(i). The initial average gray value of grid is denoted by G_0, which is corresponding to the case of no Pb^{2+} presence as shown in Fig. 4(a). With the increase of Pb^{2+}, the image becomes brighter and the value of G decreases accordingly, therefore, the relative intensity increment with the expression $(G_0\text{-}G)/G_0$ demonstrates a dynamic range of Pb^{2+}. It is noticed that, as the surface tension between the grid edges and LC molecules, some LC molecules will be adsorbed on the TEM grid edges and gather together form a random arrangement, leading to inevitable light leakages even in homeotropic LC configuration. It can be expressed by $y = 0.1893x\text{-}0.2998$, where the Pb^{2+} sensor has a broad dynamic range of 50 nM- 500 μM. In this system, the dynamic range of the Pb^{2+} is affected by concentration of DNA strand. Thus the the increase of the concentration of DNA strand might lead to wider dynamic range. The detection limit was obtained about 36.8 nM according to the 3σ criteria, where σ is the standard deviation based on calculating three parallel blank signals and M is the slope between signal and sample concentration. A similar work is reported by Mazumdar et al., where they useed the 8-17 DNA strand and AuNPs to construct an easy-to-use dipstick test for Pb^{2+} and achieved a detection limit of 500 nM [36]. Xiao et al. developed an electrochemical biosensor based on DNAzyme to detection Pb^{2+} with a detection limit of 300 nM [37]. Wang et al. demonstrated a polydiacetylene-based sensor for Pb^{2+} with a limit of 1 μM [38].

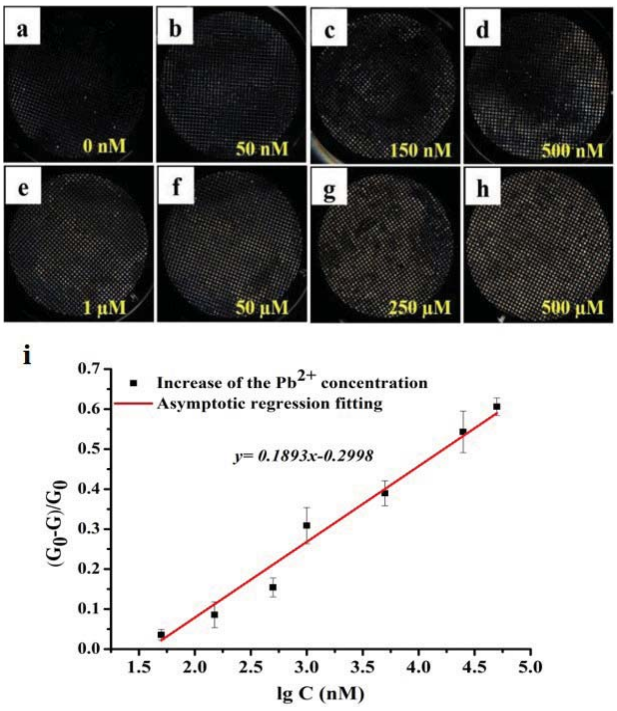

Fig. 4. The optical image under POM for Pb^{2+} sensor when the concentration of Pb^{2+} is (a) 0 nM, (b) 50 nM, (c) 150 nM, (d) 500 nM, (e) 1 μM, (f) 50 μM, (g) 250 μM, and (h) 500 μM, respectively. (i) The relationship between optical image brightness $(G_0\text{-}G)/G_0$ versus a series of Pb^{2+} concentration of from 50 nM to 500 μM.

Optics EXPRESS

Another important performance parameter of sensor in practical application is the selectivity. Figure 5 demonstrates the selectivity of Pb^{2+} sensor at presence of 100 µM Ca^{2+}, Mg^{2+}, Al^{3+}, Cd^{2+}, K^{+}, Mn^{2+}, Cu^{2+}, Zn^{2+}, Fe^{3+}, Hg^{2+}, Ag^{+} and 1 µM Pb^{2+}. It can be seen that the optical image brightness was sharply increased that was induced by addition of 1 µM Pb^{2+}, while no significant change had been observed after the addition of 100 µM other metal ions. The restoration efficiency of Pb^{2+} was about 4 times to other metal ions. This optical sensor is helpful to distinguish Hg^{2+} and Pb^{2+} as it is not easy to identify them. The system shows negligible response of Ca^{2+}, Mg^{2+}, Al^{3+}, Cd^{2+}, K^{+}, Mn^{2+}, Cu^{2+}, Zn^{2+}, Fe^{3+}, Hg^{2+}, and Ag^{+} under the similar condition. The results indicates that other metal ions aforementioned couldn't cleave the DNA strands and disturb the LC homeotropic configuration, therefore there is no much change of optical image. The result shows that the sensor possesses a remarkable high sensitivity to Pb^{2+}. This is the first time to achieve high sensitive and selective optical sensor for Pb^{2+} detection based on cleave of DNA strands induced change of liquid crystals configuration.

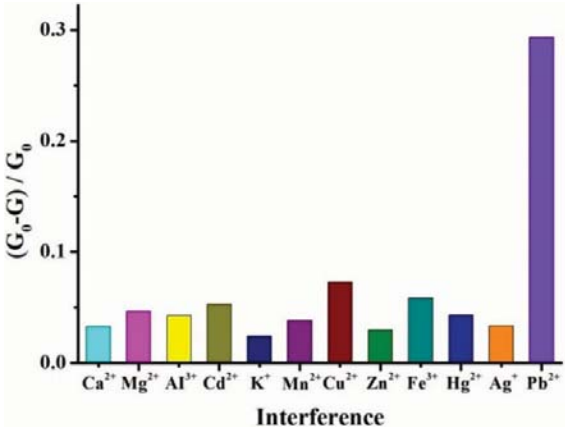

Fig. 5. Selectivity of the sensor in presence of Ca^{2+}, Mg^{2+}, Al^{3+}, Cd^{2+}, K^{+}, Mn^{2+}, Cu^{2+}, Zn^{2+}, Fe^{3+}, Hg^{2+}, Ag^{+} (100 µM) and Pb^{2+} (1 µM).

4. Conclusions

In this work, a novel liquid crystal optical sensor for detection of Pb^{2+} based on DNAzyme and its combined strand has been demonstrated. The ordered and disordered configuration of liquid crystals, induced by complementary DNA strand and catalytically cleaved DNA in presence of lead ion separately, leads to dark and bright optical image under POM. The proposed naked-eye optical sensor possesses an extremely broad detection range of Pb^{2+} from 50 nM to 500 µM, with a low detection limit about 36.8 nM. The sensor also demonstrates high selectivity of Pb^{2+} from many other metal ions. The proposal LC sensor is high selective and sensitive for Pb^{2+} detection, which provides a novel platform for other heavy metal, DNAs or antigen in biological and chemical fields by modifying sensing molecules.

Funding

National Natural Science Foundation of China (61875081); Shenzhen Science and Technology Innovation Commission (JCYJ20180305180700747).

References

1. D. Larcher and J. M. Tarascon, "Towards greener and more sustainable batteries for electrical energy storage," Nat. Chem. **7**(1), 19–29 (2015).

Optics EXPRESS

2. Y. Peng, H. Huang, Y. Zhang, C. Kang, S. Chen, L. Song, D. Liu, and C. Zhong, "A versatile MOF-based trap for heavy metal ion capture and dispersion," Nat. Commun. **9**(1), 187–196 (2018).
3. S. Bolisetty and R. Mezzenga, "Amyloid–carbon hybrid membranes for universal water purification," Nat. Nanotechnol. **11**(4), 365–371 (2016).
4. H. Y. Lee, D. R. Bae, J. C. Park, H. Song, W. S. Han, and J. H. Jung, "A selective fluoroionophore based on BODIPY-functionalized magnetic silica nanoparticles: removal of Pb^{2+} from human blood," Angew. Chem., Int. Ed. **48**(7), 1239–1243 (2009).
5. M. Sebastian and B. Mathew, "Ion imprinting approach for the fabrication of an electrochemical sensor and sorbent for lead ions in real samples using modified multiwalled carbon nanotubes," J. Mater. Sci. **53**(5), 3557–3572 (2018).
6. C. Zheng, L. Hu, X. Hou, B. He, and G. Jiang, "Headspace solid-phase microextraction coupled to miniaturized microplasma optical emission spectrometry for detection of mercury and lead," Anal. Chem. **90**(6), 3683–3691 (2018).
7. Y. Wang, S. Gao, X. Zang, J. Li, and J. Ma, "Graphene-based solid-phase extraction combined with flame atomic absorption spectrometry for a sensitive determination of trace amounts of lead in environmental water and vegetable samples," Anal. Chim. Acta **716**, 112–118 (2012).
8. R. A. Zounr, M. Tuzen, and M. Y. Khuhawar, "A simple and green deep eutectic solvent based air assisted liquid phase microextraction for separation, preconcentration and determination of lead in water and food samples by graphite furnace atomic absorption spectrometry," J. Mol. Liq. **259**, 220–226 (2018).
9. G. Pelossof, R. Tel-Vered, and I. Willner, "Amplified surface plasmon resonance and electrochemical detection of Pb^{2+} ions using the Pb^{2+}-dependent DNAzyme and hemin/G-quadruplex as a label," Anal. Chem. **84**(8), 3703–3709 (2012).
10. W. Yun, D. Cai, J. Jiang, P. Zhao, Y. Huang, and G. Sang, "Enzyme-free and label-free ultra-sensitive colorimetric detection of Pb^{2+} using molecular beacon and DNAzyme based amplification strategy," Biosens. Bioelectron. **80**, 187–193 (2016).
11. Z. Huang, J. Chen, Z. Luo, X. Wang, and Y. Duan, "Label-free and Enzyme-free Colorimetric Detection of Pb^{2+} Based on RNA-Cleavage and Annealing-Accelerated Hybridization Chain Reaction," Anal. Chem. **91**(7), 4806–4813 (2019).
12. T. Li, S. Dong, and E. Wang, "A lead (II)-driven DNA molecular device for turn-on fluorescence detection of lead (II) ion with high selectivity and sensitivity," J. Am. Chem. Soc. **132**(38), 13156–13157 (2010).
13. M. Baghayeri, A. Amiri, B. Maleki, Z. Alizadeh, and O. Reiser, "A simple approach for simultaneous detection of cadmium (II) and lead (II) based on glutathione coated magnetic nanoparticles as a highly selective electrochemical probe," Sens. Actuators, B **273**, 1442–1450 (2018).
14. Y. Wang, G. Zhao, Q. Zhang, H. Wang, Y. Zhang, W. Cao, N. Zhang, B. Du, and Q. Wei, "Electrochemical aptasensor based on gold modified graphene nanocomposite with different morphologies for ultrasensitive detection of Pb^{2+}," Sens. Actuators, B **288**, 325–331 (2019).
15. R. R. Shah and N. L. Abbott, "Principles for measurement of chemical exposure based on recognition-driven anchoring transitions in liquid crystals," Science **293**(5533), 1296–1299 (2001).
16. K. Goossens, K. Lava, C. W. Bielawski, and K. Binnemans, "Ionic liquid crystals: versatile materials," Chem. Rev. **116**(8), 4643–4807 (2016).
17. P. K. Mukherjee, "Influence of carbon nanotubes in antiferroelectric liquid crystals," Soft Mater. **17**(4), 321–327 (2019).
18. H. Iino, T. Usui, and J. i. Hanna, "Liquid crystals for organic thin-film transistors," Nat. Commun. **6**(1), 6828 (2015).
19. X. Wang, D. S. Miller, E. Bukusoglu, J. J. De Pablo, and N. L. Abbott, "Topological defects in liquid crystals as templates for molecular self-assembly," Nat. Mater. **15**(1), 106–112 (2016).
20. I. Pani, D. Sharma, and S. K. Pal, "Liquid Crystals as Sensitive Reporters of Lipid-Protein Interactions," Gen. Chem. **4**(2), 20180012 (2018).
21. A. D. Price and D. K. Schwartz, "DNA hybridization-induced reorientation of liquid crystal anchoring at the nematic liquid crystal/aqueous interface," J. Am. Chem. Soc. **130**(26), 8188–8194 (2008).
22. S. Sridharamurthy, K. Cadwell, N. Abbott, and H. Jiang, "A microstructure for the detection of vapor-phase analytes based on orientational transitions of liquid crystals," Smart Mater. Struct. **17**(1), 012001 (2008).
23. K. D. Cadwell, M. E. Alf, and N. L. Abbott, "Infrared spectroscopy of competitive interactions between liquid crystals, metal salts, and dimethyl methylphosphonate at surfaces," J. Phys. Chem. B **110**(51), 26081–26088 (2006).
24. S. Sivakumar, K. L. Wark, J. K. Gupta, N. L. Abbott, and F. Caruso, "Liquid crystal emulsions as the basis of biological sensors for the optical detection of bacteria and viruses," Adv. Funct. Mater. **19**(14), 2260–2265 (2009).
25. G. R. Han, Y. J. Song, and C. H. Jang, "Label-free detection of viruses on a polymeric surface using liquid crystals," Colloids Surf., B **116**, 147–152 (2014).
26. S. H. Yoon, K. C. Gupta, J. S. Borah, S. Y. Park, Y. K. Kim, J. H. Lee, and I. K. Kang, "Folate ligand anchored liquid crystal microdroplets emulsion for in vitro detection of KB cancer cells," Langmuir **30**(35), 10668–10677 (2014).
27. R. Manda, V. Dasari, P. Sathyanarayana, M. Rasna, P. Paik, and S. Dhara, "Possible enhancement of physical properties of nematic liquid crystals by doping of conducting polymer nanofibres," Appl. Phys. Lett. **103**(14), 141910 (2013).
28. C. H. Chen, Y. C. Lin, H. H. Chang, and A. S. Y. Lee, "Ligand-doped liquid crystal sensor system for detecting mercuric ion in aqueous solutions," Anal. Chem. **87**(8), 4546–4551 (2015).

Optics EXPRESS

29. X. H. Zhao, R. M. Kong, X. B. Zhang, H. M. Meng, W. N. Liu, W. Tan, G. L. Shen, and R. Q. Yu, "Graphene–DNAzyme based biosensor for amplified fluorescence "turn-on" detection of Pb^{2+} with a high selectivity," Anal. Chem. **83**(13), 5062–5066 (2011).
30. A. K. Brown, J. Li, C. M. B. Pavot, and Y. Lu, "A lead-dependent DNAzyme with a two-step mechanism," Biochemistry **42**(23), 7152–7161 (2003).
31. T. Li, E. Wang, and S. Dong, "Lead (II)-induced allosteric G-quadruplex DNAzyme as a colorimetric and chemiluminescence sensor for highly sensitive and selective Pb^{2+} detection," Anal. Chem. **82**(4), 1515–1520 (2010).
32. B. Zhang, L. Lu, Q. Hu, F. Huang, and Z. Lin, "ZnO nanoflower-based photoelectrochemical DNAzyme sensor for the detection of Pb^{2+}," Biosens. Bioelectron. **56**, 243–249 (2014).
33. X. Niu, Y. Zhong, R. Chen, F. Wang, Y. Liu, and D. Luo, "A "turn-on" fluorescence sensor for Pb^{2+} detection based on graphene quantum dots and gold nanoparticles," Sens. Actuators, B **255**, 1577–1581 (2018).
34. J. Chen, X. Zhou, and L. Zeng, "Enzyme-free strip biosensor for amplified detection of Pb^{2+} based on a catalytic DNA circuit," Chem. Commun. **49**(10), 984–986 (2013).
35. H. Wei, B. Li, J. Li, S. Dong, and E. Wang, "DNAzyme-based colorimetric sensing of lead (Pb^{2+}) using unmodified gold nanoparticle probes," Nanotechnology **19**(9), 095501 (2008).
36. D. Mazumdar, J. Liu, G. Lu, J. Zhou, and Y. Lu, "Easy-to-use dipstick tests for detection of lead in paints using non-cross-linked gold nanoparticle–DNAzyme conjugates," Chem. Commun. **46**(9), 1416–1418 (2010).
37. Y. Xiang, A. Tong, and Y. Lu, "Abasic site-containing DNAzyme and aptamer for label-free fluorescent detection of Pb^{2+} and adenosine with high sensitivity, selectivity, and tunable dynamic range," J. Am. Chem. Soc. **131**(42), 15352–15357 (2009).
38. M. Wang, F. Wang, Y. Wang, W. Zhang, and X. Chen, "Polydiacetylene-based sensor for highly sensitive and selective Pb^{2+} detection," Dyes Pigm. **120**, 307–313 (2015).